J. Phys. D: Appl. Phys. **40** (2007) 1408–1415 doi:10.1088/0022-3727/40/5/014

Design and operation of a supersonic flow cavity for a non-self-sustained electric discharge pumped oxygen–iodine laser

A Hicks, S Tirupathi, N Jiang, Yu Utkin, W R Lempert, J W Rich and I V Adamovich

Nonequilibrium Thermodynamics Laboratories, Department of Mechanical Engineering, The Ohio State University, Columbus, OH, USA

Received 26 October 2006, in final form 5 January 2007
Published 16 February 2007
Online at stacks.iop.org/JPhysD/40/1408

Abstract
The paper presents results of a high-pressure, non-self-sustained crossed discharge–$M = 3$ supersonic laser cavity operation. A stable and diffuse pulser–sustainer discharge in O_2–He flows is generated at pressures of up to $P_0 = 120$ Torr and discharge powers of up to 2.1 kW. The reduced electric field in the dc sustainer discharge ranges from 0.6×10^{-16} to 1.2×10^{-16} V cm^2. Singlet delta oxygen (SDO) yield in the discharge, up to 5.0–5.7% at the flow temperatures of 400-420 K, was inferred from the integrated intensity of the (0,0) band of the $O_2(a\,^1\Delta \rightarrow X\,^3\Sigma)$ infrared emission spectra calibrated using a blackbody source. The yield increases with the discharge power and remains nearly independent of the O_2 fraction in the mixture (in the 10–20% range). Static pressure and temperature measurements in the supersonic cavity show that a steady-state $M = 3$ flow in the cavity can be sustained for up to 20 s, at the flow temperature of $T = 120 \pm 15$ K. The results suggest that the measured SDO yield exceeds the threshold yield at the cavity temperature by up to a factor of 2.5. PLIF iodine vapour visualization in the supersonic cavity, which showed the presence of large-scale structures, suggests the need to improve iodine vapour mixing with the main oxygen–helium flow.

(Some figures in this article are in colour only in the electronic version)

1. Introduction

Over the recent years, development of an electrically pumped oxygen–iodine laser scalable to high powers has attracted considerable attention [1–13]. One of the main goals of this work is achieving singlet delta oxygen (SDO) yield in a low-temperature gas discharge plasma, exceeding threshold yield for positive gain in an oxygen–iodine mixture, $Y_{th} = [1 + 1.5\exp(403/T)]^{-1}$ [14]. The strong temperature dependence of the threshold yield suggests that the flow temperature needs to be reduced before it enters the laser cavity, using a rapid supersonic expansion. Indeed, recent experiments in an RF discharge in O_2–He mixtures at $P = 10$ Torr, followed by a $M = 2$ expansion demonstrated positive gain on a 1315 nm iodine atom transition [6], cw lasing with a 220 mW output power at the cavity temperature of $T = 190$ K [10] and laser output power increase up to 1.5 W [13]. Using higher Mach number, lower temperature expansion, which would further lower the threshold yield, requires operating at rather high discharge pressures. For a $M = 3$ cavity pressure of $P = 2$–4 Torr, the stagnation pressure in a 10% O_2–He flow should be $P_0 = 65$–130 Torr. Also, to optimize SDO yield in the plasma, the discharge should operate at reduced electric field (E/N) values where the energy input into the $O_2(a\,^1\Delta)$ state is maximum. It is well known that this maximum is achieved at low E/N values, $E/N < 10$ Td [1, 3, 4], which suggests the use of a non-self-sustained electric discharge, where an external ionization source is uncoupled from the applied electric field. In these discharges, the electric field can be independently varied across a wide range. An additional advantage of such discharges is that they remain stable at high pressures and energy inputs [15].

Report Documentation Page

Form Approved
OMB No. 0704-0188

1. REPORT DATE **JAN 2007**	2. REPORT TYPE	3. DATES COVERED **00-00-2007 to 00-00-2007**

4. TITLE AND SUBTITLE
Design and operation of a supersonic flow cavity for a non-self-sustained electric discharge pumped oxygen-iodine laser

5a. CONTRACT NUMBER

5b. GRANT NUMBER

5c. PROGRAM ELEMENT NUMBER

6. AUTHOR(S)

5d. PROJECT NUMBER

5e. TASK NUMBER

5f. WORK UNIT NUMBER

7. PERFORMING ORGANIZATION NAME(S) AND ADDRESS(ES)
Ohio State University,Department of Mechanical Engineering,Columbus,OH,43202

8. PERFORMING ORGANIZATION REPORT NUMBER

9. SPONSORING/MONITORING AGENCY NAME(S) AND ADDRESS(ES)

10. SPONSOR/MONITOR’S ACRONYM(S)

11. SPONSOR/MONITOR’S REPORT NUMBER(S)

12. DISTRIBUTION/AVAILABILITY STATEMENT
Approved for public release; distribution unlimited

13. SUPPLEMENTARY NOTES

14. ABSTRACT
The paper presents results of a high-pressure, non-self-sustained crossed discharge?M = 3 supersonic laser cavity operation. A stable and diffuse pulser?sustainer discharge in O2?He flows is generated at pressures of up to P0 = 120 Torr and discharge powers of up to 2.1kW. The reduced electric field in the dc sustainer discharge ranges from 0.6 ?10−16 to 1.2 ?10−16 Vcm2. Singlet delta oxygen (SDO) yield in the discharge, up to 5.0?5.7% at the flow temperatures of 400-420 K, was inferred from the integrated intensity of the (0,0) band of the O2(a 1 → X 3) infrared emission spectra calibrated using a blackbody source. The yield increases with the discharge power and remains nearly independent of the O2 fraction in the mixture (in the 10?20% range). Static pressure and temperature measurements in the supersonic cavity show that a steady-state M = 3 flow in the cavity can be sustained for up to 20 s, at the flow temperature of T = 120 ? 15 K. The results suggest that the measured SDO yield exceeds the threshold yield at the cavity temperature by up to a factor of 2.5. PLIF iodine vapour visualization in the supersonic cavity, which showed the presence of large-scale structures, suggests the need to improve iodine vapour mixing with the main oxygen?helium flow.

15. SUBJECT TERMS

16. SECURITY CLASSIFICATION OF:			17. LIMITATION OF ABSTRACT	18. NUMBER OF PAGES	19a. NAME OF RESPONSIBLE PERSON
a. REPORT **unclassified**	b. ABSTRACT **unclassified**	c. THIS PAGE **unclassified**	**Same as Report (SAR)**	**8**	

Standard Form 298 (Rev. 8-98)
Prescribed by ANSI Std Z39-18

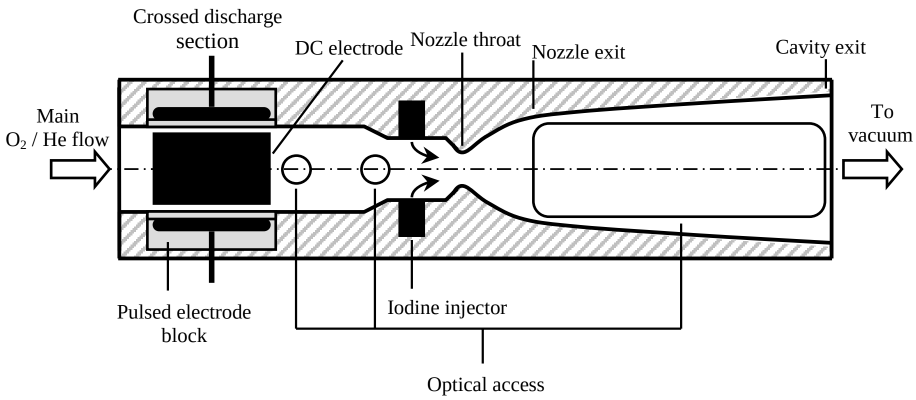

Figure 1. Schematic of the discharge section / nozzle / laser cavity assembly.

The approach used in the present work employs two overlapping discharges, a repetitively pulsed discharge and a dc sustainer discharge. In this approach, uniform ionization is produced by high voltage, high repetition rate ionizing pulses, with the pulse duration too short to allow ionization instability development. The pulse repetition rate is sufficiently high to avoid complete plasma decay between the pulses. The dc voltage is too low to produce additional ionization, so that the decaying plasma remains stable. The dc voltage, tailored to maximize the energy input into the $O_2(a\,^1\Delta)$ state, couples power to the plasma. This method, first demonstrated by Hill [16], has been previously used to develop a high power, fast flow CO_2 laser [15, 17]. Recent experiments at the Nonequilibrium Thermodynamics Group using the crossed discharge [12] showed that, indeed, it produced stable and diffuse plasmas in oxygen–helium flows, at high pressures and higher energy loadings, at least up to $P = 0.5$ atm and 1200 W, respectively. The reduced electric field in the crossed discharge varied from $E/N = 0.3 \times 10^{-16}$ V cm^2 to $E/N = 0.65 \times 10^{-16}$ V cm^2, which is significantly lower than E/N in self-sustained discharges and close to the theoretically predicted optimum value for $O_2(a\,^1\Delta)$ excitation [12]. Flow temperature rise in the discharge was rather modest, $\Delta T = 65$–165 K. SDO yield at these conditions was 1.7–4.4%. The crossed discharge technique has also been used in our recent experiments on low-temperature MHD flow control [18, 19] and on non-equilibrium plasma ignition [20].

The main objective of the present paper is to test the operation of a modified crossed discharge SDO generator together with the iodine injection system and supersonic nozzle/laser cavity assembly designed for an electric discharge pulsed oxygen–iodine laser.

2. Experimental

The experiments have been conducted at an electrically pumped, supersonic flow oxygen–iodine laser facility currently under development at the Nonequilibrium Thermodynamics Laboratories at Ohio State. A schematic of the experiment is shown in figure 1. A premixed helium/oxygen flow is produced by mixing helium with a 50%/50% mixture of helium and oxygen. The helium cylinders are stacked to increase the overall available operation time. The flow is delivered to the test section via a 1 inch diameter, 15 ft long supply line.

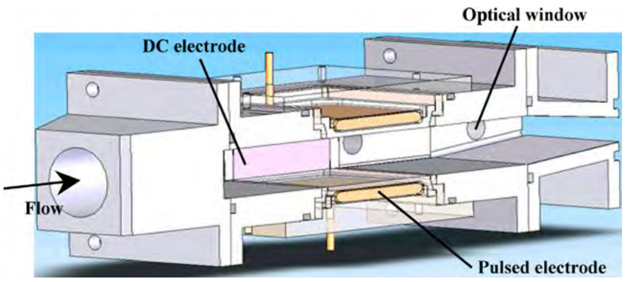

Figure 2. Sectioned view of the crossed discharge test section.

The discharge section, the overall view of which is shown in figure 2, is made of acrylic plastic and has a rectangular inner cross section of 5 cm × 2 cm. Compared with our previous paper [12], the discharge section height is increased from 1 to 2 cm to increase the flow residence time in the discharge at the same mass flow rate, which is expected to result in higher SDO yield [12].

Two rectangular dc electrodes, each 5 cm long and 2 cm wide, and two square-shaped pulsed electrodes, 5 cm × 5 cm, are flush-mounted in the side walls and in the top/bottom walls of the discharge section, respectively (see figure 2). The dc electrodes are made of copper and are exposed to the flow. Each pulsed electrode plate, also made of copper, is sandwiched between a 1 mm thick macor ceramic plate on the flow side and macor ceramic housing on the opposite side (see figure 2). To prevent corona discharge formation in the air pockets between the ceramic plate, the copper electrode and the recessed ceramic housing, this space is filled by a self-hardening dielectric compound (silicon rubber). Both sets of electrodes are located at the same streamwise location to form a crossed pulser/dc sustainer discharge, as shown in figure 2. The overall length of the discharge section is about 12 cm, with the crossed discharge length of 5 cm.

The pulsed electrodes are powered by a Chemical Physics Technologies custom designed high voltage (20–25 kV), short pulse duration (10–20 ns), high pulse repetition rate (up to 50 kHz) plasma generator. The duty cycle of the repetitively pulsed discharge is very low, $\sim 1/1000$. The pulser has a low-voltage transistor–transistor logic (TTL) pulse output synchronized with the main high voltage pulses, which can be used to trigger the dc power supply and the diagnostic equipment. The pulse voltage and current are measured using a Tektronix P6015A high voltage probe, a low-capacitance resistive current probe and a LeCroy Wavepro 7100A digital oscilloscope. In the present experiments, the pulser was operated at a pulse repetition rate of $\nu = 40$ kHz. The dc sustainer electrodes are powered by a Glassman high current dc power supply (5 kV, 2 A, 10 kW max), operated in the voltage-stabilized mode. Adjustable high-power ballast resistors (Powerohm, 1050 W) are connected in series with the dc power supply to limit the maximum sustainer current. In all present experiments, the ballast resistance has been set at $R = 1.0\,\mathrm{k}\Omega$. The dc sustainer current is measured using a Tektronix A6303 current probe with a Tektronix AM503B amplifier and a LeCroy Wavepro 7100A digital oscilloscope.

The discharge section is followed by the iodine injection channel, a converging–diverging nozzle, and a supersonic laser cavity (see figure 1). Iodine vapour is added into the main oxygen–helium flow using an iodine metering/delivery system developed by Physical Sciences Inc. (PSI). Iodine vapour is produced by flowing helium carrier gas over a bed of heated iodine crystals. Iodine concentration in the carrier flow is measured by molecular iodine continuum absorption at 488 nm in an absorption cell [21]. The system is capable of adding up to 70 μmol s^{-1} of iodine vapour to helium carrier flow, at the carrier flow rate of up to 60 mmol s^{-1}. The iodine vapour/helium mixture is delivered to the test section through two heated 1/4 inch diameter stainless steel lines and injected into the main flow through two stainless steel injection blocks located upstream of the nozzle throat, where the main flow Mach number is $M \sim 0.5$ (see figure 1). Every injector block has sixteen 1.25 mm diameter injection holes arranged in a single row across the flow and is heated by four cartridge heaters. The injectors are estimated to be sonic since the pressure ratio across the injection block is approximately 4 to 10 (iodine vapour/helium mixture delivery pressure of 400-500 Torr and the flow static pressure at the injector location of 50–100 Torr).

The contoured $M = 3$ nozzle throat dimensions are 5 cm × 0.32 cm and the nozzle exit dimensions are 5 cm × 1 cm. The discharge section/nozzle throat area ratio, $A/A^* = 6.25$, corresponds to the discharge section Mach number of $M \sim 0.1$ for $\gamma = 1.625$, so that the discharge section serves as the nozzle plenum. Therefore, measuring the discharge section pressure (i.e. the stagnation pressure) in helium and in an oxygen–helium mixture allows inference of both the mass flow rate through the test section and mole fractions of oxygen and helium. The stagnation pressure and the mixture composition can be varied independently. The top and bottom walls of the supersonic section, which will be a part of the transverse laser cavity, are diverging at 1.5° each to provide the boundary layer relief, as shown in figure 1. Plastic inserts, transparent for both visible and 1.3 μm infrared radiation, are flush-mounted in the side walls of the supersonic section and span its entire length and height from the nozzle exit, providing optical access to the entire supersonic flow (see figure 1). Additional BK-7 glass optical access windows are located downstream of the discharge section, as shown in figures 1 and 2.

Visible and infrared emission spectroscopy measurements have been conducted using a 0.5 m monochromator, 600 g mm^{-1} grating blazed at 1 μm, and a Roper Scientific liquid nitrogen-cooled 1D array 1024 pixel InGaAs PDA

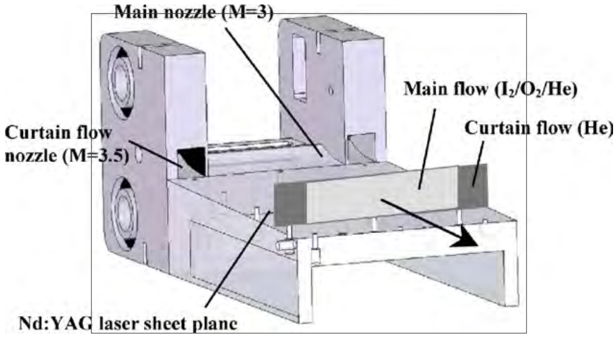

Figure 3. Bottom part of the nozzle/laser cavity assembly with the schematic of the $M = 3$ core flow and $M = 3.5$ curtain flows in the supersonic cavity. Three axial rows of static pressure taps are shown along the bottom cavity wall.

OMA V camera. The emission signal was collected using a Thor Labs 1 m long fibre optic bundle with a 1 inch diameter collimator on the collection end. The collimator was positioned in front of a window (either in the discharge section wall or in the supersonic cavity wall), and the opposite end of the fibre optic bundle was placed in front of the spectrometer slit. The use of the fibre optic link greatly improved the alignment of the optical diagnostics system. The $O_2(a\,^1\Delta)$ concentration in the discharge afterglow and the SDO yield were evaluated by absolute calibration of the fibre optics/OMA/CCD camera signal collection system using an Infrared Systems calibrated blackbody source IR-564. The Einstein coefficient for spontaneous emission of $O_2(a\,^1\Delta)$ was taken to be $A = 2.2 \times 10^{-4}\,\mathrm{s}^{-1}$ [22, 23]. In the present experiments, the SDO emission signal was collected through an optical window approximately 8 cm downstream of the discharge (see figures 1 and 2). The flow residence time between the end of the discharge and the optical window was about 1 ms. In the present paper, as in our previous paper [12], the SDO yield is defined as follows, $Y_{\mathrm{SDO}} = [O_2(a\,^1\Delta)]/[O_2]$, where $[O_2(a\,^1\Delta)]$ is SDO number density and $[O_2]$ is the initial oxygen number density.

Iodine vapour mixing visualization in the supersonic test section is performed using an I_2 planar laser induced fluorescence (PLIF) imaging technique. For this, we used the second harmonic output of a Continuum broadband ‘Mini’ Q-switched Nd : YAG laser at 532 nm to pump a variety of rotational transitions within the $I_2\left(X\,^1\Sigma_g^+, v = 3 \rightarrow B\,^3\Pi_{\mathrm{ou}}^+, v = 0\right)$ vibrational band. The $\sim$ 5 mJ/pulse output of the laser, operated at a 10 Hz pulse repetition rate, is formed into a relatively thick ($\sim$1 mm) sheet using a 25 mm focal length negative cylindrical lens. As schematically shown in figure 3, the laser sheet is directed across the flow approximately 5 cm downstream of the nozzle exit plane, orthogonally to the flow direction. The fluorescence signal was captured using a GEN IV near IR sensitive ICCD camera, at an angle of approximately 45° to the sheet laser sheet. The intensifier gate was delayed $\sim$50 ns from the laser pulse in order to eliminate Mie scattering and stray light and then turned on for $\sim$2 μs to capture the I_2 fluorescence.

In the future, we are planning to attach helium-purged laser resonator arms on both sides of the supersonic test section. To prevent the laser mirrors from iodine deposits during the

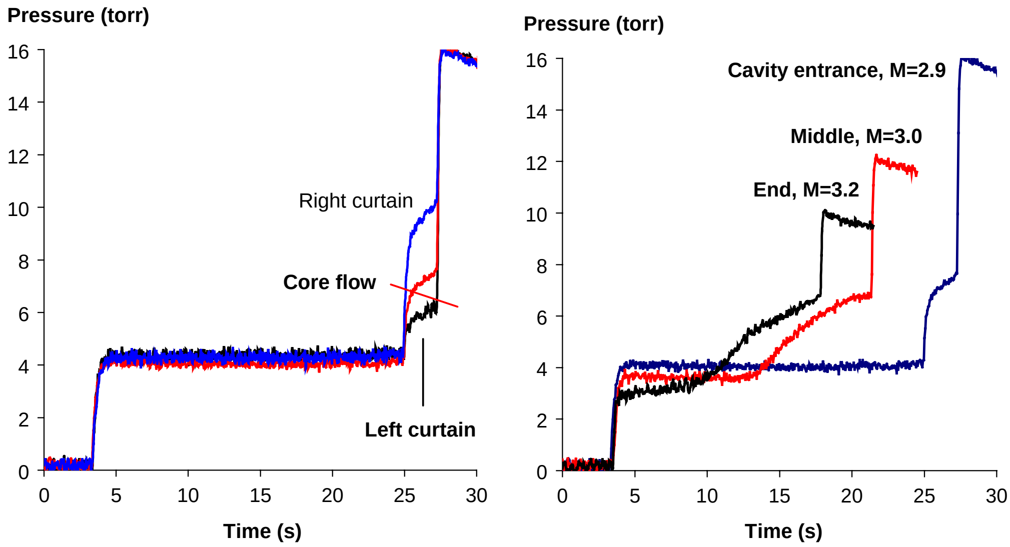

Figure 4. (left) static pressure measurements at the core flow and two curtain flow nozzle exits (see figure 3); (right) static pressure measurements at three different streamwise locations along the centerline of the core flow. $P_0 = 111$ Torr, $M = 2.9$.

operation, two helium curtain flows are injected into the cavity on both sides of the main $M = 3$ flow using two $M = 3.5$ curtain flow nozzles 1 cm wide each, as shown in figure 3. The main flow nozzle exit and the curtain flow nozzle exits are located at the same streamwise location (see figure 3). Three rows of static pressure taps (one row along the centreline, one row along each curtain flows, five taps per row) are located in the bottom wall of the cavity, as shown in figure 3, to monitor the supersonic flow quality.

In the present experiments, the test section total pressure was in the range from $P_0 = 60$ to 120 Torr and remained constant during the run. At the baseline conditions of $P_0 = 120$ Torr, 10% O_2 in He, the flow rates of O_2 and He are 44 mmol s^{-1} and 400 mmol s^{-1}, respectively, at the total mass flow rate of 3.0 g s^{-1}. To reduce the time needed for starting and pressure matching among the four flows (main helium, main 50–50% oxygen–helium mixture, iodine vapour/helium mixture and curtain flow helium), the preset flows can be quickly started and stopped by using remotely controlled solenoid valves. Downstream of the supersonic cavity, a 4 inch diameter shutoff ball valve allowed test section removal while keeping the dump tank under vacuum. The tank volume is approximately 1000 ft^3. Between the runs, the tank is pumped down to approximately 0.1 Torr using a Stokes 212-H 150 cfm vacuum pump. During the run, the tank pressure increased by a few Torr.

3. Results and discussion

Figure 4 shows the results of flow static pressure measurements in the slightly diverging supersonic test section, in a 10% O_2–He flow at a plenum pressure of $P_0 = 111$ Torr. During these measurements, the crossed discharge in the nozzle plenum was turned off. From figure 4(*a*), it can be seen that the static pressures among the core flow and two curtain flows (on the left and on the right) are quickly matched, within about a second. The core flow Mach number at the nozzle exit, determined from the quasi-one-dimensional isentropic compressible flow theory at $\gamma = 1.625$, is $M = 2.9$. From figure 4(*b*), one can also see that a steady-state $M = 2.9$–3.2 flow in the test section can be sustained from 5 to 20 s, depending on the axial location. The static pressure somewhat decreases and the Mach number somewhat increases in the direction of the flow because of the slight divergence in the test section walls (see figure 1). The flow Mach numbers and the run times measured at a lower plenum pressure, $P_0 = 60$ Torr, are very close to the results at $P_0 = 111$ Torr. These results have been obtained without using a diffuser downstream of the supersonic cavity.

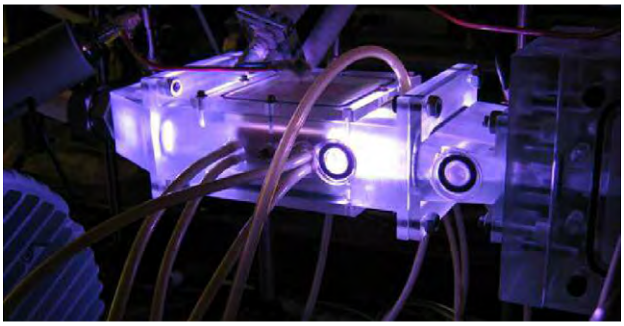

Figure 5. Photograph of a pulsed discharge in the nozzle plenum at $P_0 = 120$ Torr.

After the flow is started and the test section pressure is stabilized, the crossed discharge is initiated by starting the high voltage, high repetition rate pulse sequence. Both the dc power supply and the optical diagnostics system are turned on shortly thereafter and are turned off before the pulser is turned off. Figure 5 shows a photograph of the discharge section with pulsed discharge in operation at $P_0 = 120$ Torr. High voltage, short duration pulses produce ionization in the test section, and the relatively low sustainer voltage draws current across the test section between the pulses, while electron density is decaying due to electron recombination and attachment. Figure 6 shows a typical single pulse voltage and current traces obtained in a 10% O_2–He flow at $P_0 = 60$ Torr. Pulse peak voltage is 15 kV and pulse FWHM is 25 ns. At these conditions, the peak pulse

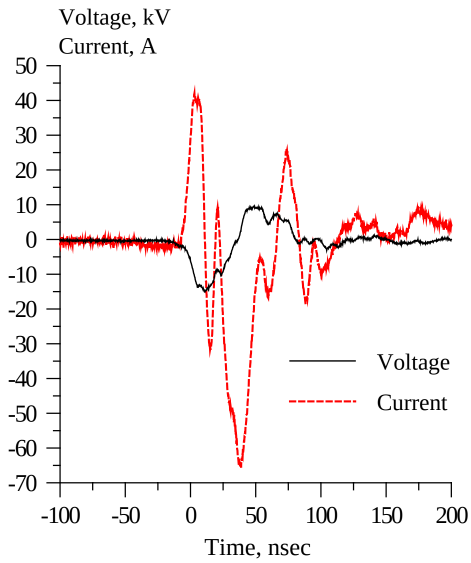

Figure 6. Typical single-pulse discharge oscillogram. Pulse peak voltage 15 kV, pulse FWHM 25 ns 10% O_2 in helium, $P = 60$ Torr.

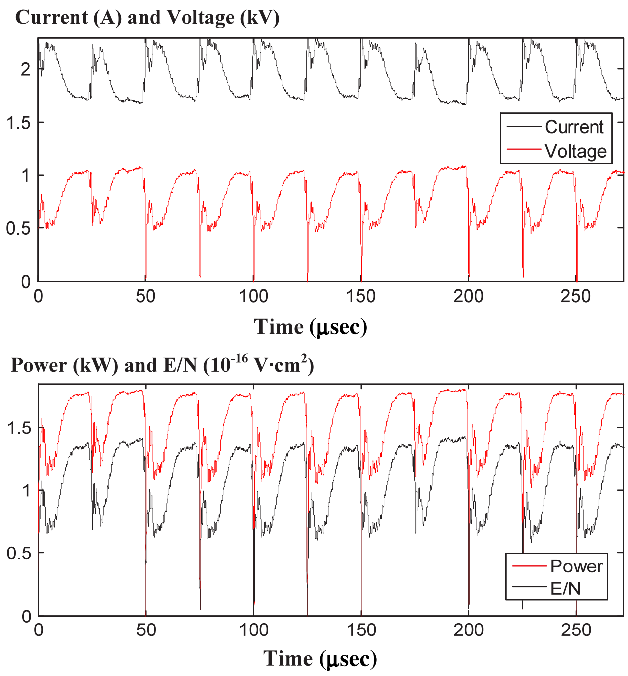

Figure 7. Current, voltage, power and E/N in a dc sustainer discharge. 10% O_2/90% He mixture, $P_0 = 60$ Torr, $U = 2.5$ kV, pulse repetition rate $\nu = 40$ kHz.

current is approximately 65 A and the pulse energy coupled to the flow, calculated by integrating the product of the voltage and current waveforms, is 2.1 mJ. Typical single pulse energies are in the 2–3 mJ range, which at the pulse repetition rate of $\nu = 40$ kHz corresponds to the time-averaged power added to the flow of 80–120 W.

For the measurements reported in the present paper, a typical run time with the crossed discharge turned on was from 5 to 15 s. Figure 7 shows oscillograms of the sustainer current and voltage as well as of the sustainer discharge power coupled to the flow and the estimated reduced electric field, E/N, in the

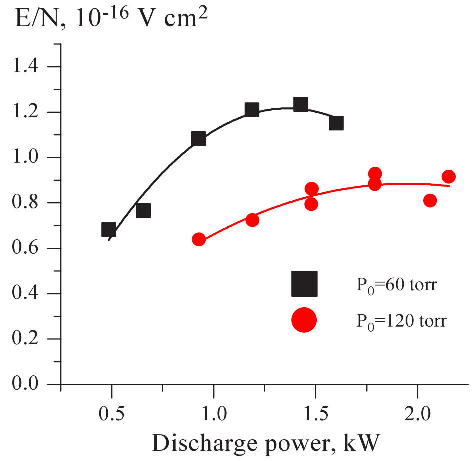

Figure 8. Time-averaged reduced electric field versus time-averaged sustainer discharge power. 10% O_2 in helium.

crossed discharge in a 10% O_2–He flow at $P_0 = 60$ Torr and pulse repetition rate of $\nu = 40$ kHz. In figure 7, the dc power supply voltage was $U_{PS} = 2.5$ kV with the ballast resistor of $R = 1.0$ kΩ. The reduced electric field in figure 7 is evaluated based on the flow number density at room temperature and neglecting the cathode voltage fall in the sustainer discharge. From figure 7, it can be seen that the sustainer current and voltage vary from $I = 2.2$ A to $U = 1.75$ A and from $U = 1.0$ kV to $U = 0.5$ kV, respectively. The discharge power and the reduced electric field at these conditions are 1.1–1.7 kW and $(0.7–1.3)\times10^{-16}$ V cm^2, respectively. The crossed discharge at these conditions remained non-self-sustained. Applying dc voltages higher than $U_{PS} = 2.75$ kV at a pressure of 60 Torr made the dc discharge self-sustained, which resulted in instability development. At these conditions, SDO emission signal significantly decreased, which demonstrated the importance of operating the high-pressure dc discharge in the non-self-sustained mode.

Figure 8 shows time-averaged values of the reduced electric field in the sustainer discharge in a 10% O_2– 90% He mixture at $P_0 = 60$ and 120 Torr, plotted against the time-averaged discharge power. The discharge power was varied by changing the dc power supply voltage. It can be seen that the sustainer power coupled to the flow at $P_0 = 60$ Torr and 120 Torr ranges from 0.5 kW to 1.6 kW and from 0.9 kW to 2.1 kW, respectively. This is considerably higher than has been previously achieved in our previous experiments in the same mixture but at a shorter flow residence time, only up to 0.9 kW at $P_0 = 120$ Torr [12]. The experiments [12] have been conducted in a smaller cross section test section, 5 cm × 1 cm. From figure 8, one can also see that the reduced electric field in the sustainer discharge increases with the discharge power. The present results at $P_0 = 120$ Torr are consistent with our previous measurements at the same pressure but at lower discharge powers [12], $E/N = 0.65 \times 10^{-16}$ V cm^2 at 0.9 kW.

As in our previous paper [12], the flow temperature in the discharge was determined from a partially rotationally resolved (0,0) band of the $O_2(b\,^1\Sigma \rightarrow X^3\Sigma)$ emission spectra with the band centre at 762 nm. The same approach was used to determine the temperature in the $M = 3$ supersonic test

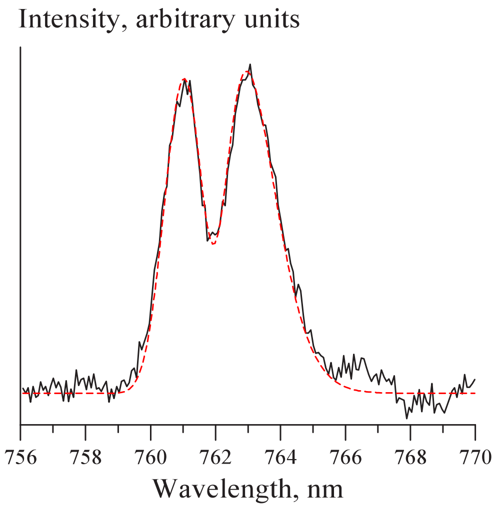

Figure 9. Experimental (solid line) and synthetic (dashed line) $O_2(b^1\Sigma \to X^3\Sigma)$ emission spectra measured in the supersonic cavity. 10% O_2 in helium, $P_0 = 60$ Torr, $P = 1.9$ Torr, $U_{PS} = 2.5$ kV, $T = 120$ K.

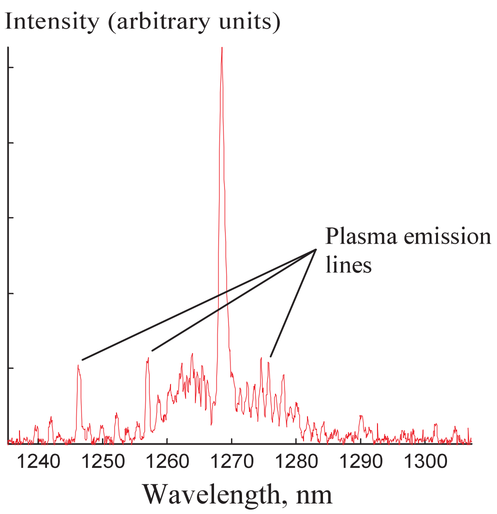

Figure 10. Typical $O_2(a^1\Delta \to X^3\Sigma)$ emission spectrum measured in the discharge section. 10% O_2 in helium, $P_0 = 60$ Torr, $U_{PS} = 2.5$ kV.

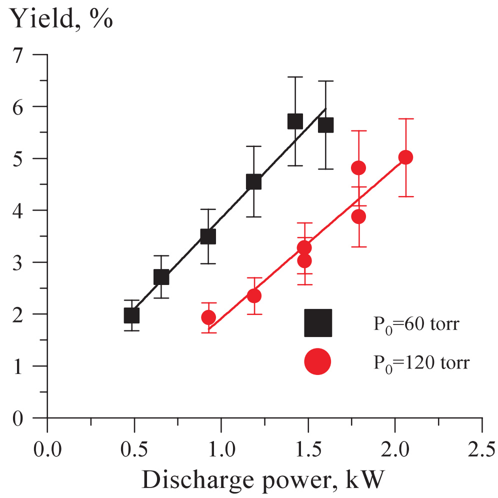

Figure 11. Summary of the $O_2(a^1\Delta)$ yield measurements versus sustainer discharge power in 10% O_2–He flows.

section. Figure 9 shows a typical $O_2(b\,^1\Sigma \to X^3\Sigma)$ emission spectrum measured at the end of the supersonic test section (see figure 1), at $P_0 = 60$ Torr, $P = 1.9$ Torr ($M = 3.0$), and the discharge power of 1.4 kW. In this case, the synthetic spectrum indicates the flow temperature of $T = 120 \pm 15$ K (see figure 9). At $P_0 = 120$ Torr, at the discharge power of 2.1 kW, the temperature was essentially the same, $T = 120 \pm 15$ K. This shows that the temperature in the supersonic cavity is in close agreement with the prediction of quasi-one dimensional compressible flow theory at $\gamma = 1.625$ and $M = 3.0$, $T \approx 110$ K.

Figure 10 shows a typical $O_2(a\,^1\Delta \to X^3\Sigma)$ infrared emission spectrum, (0,0) band with the band centre at 1.268 μm, in a 10% O_2–He mixture at $P_0 = 60$ Torr. The spectrum in figure 10 is shown after subtracting a nearly flat blackbody emission baseline from the raw infrared signal. In figure 10, one can see atomic emission lines overlapped with the SDO emission band. As in [12], the SDO yield was inferred from the experimental infrared emission spectra using blackbody calibration and flow temperatures obtained from the $O_2(b\,^1\Sigma \to X^3\Sigma)$ spectra, such as shown in figure 10. During the calibration, both the signal collection volume sampled by the fibre optics collimator and contributions of different parts of the collection volume into the overall SDO signal were determined.

Figure 11 plots experimental SDO yield versus the sustainer discharge power, measured in 10% O_2–He flows at two different discharge pressures, $P_0 = 60$ and 120 Torr. The error bars in figure 11 indicate a combined uncertainty in the Einstein coefficient for spontaneous emission for the $O_2(a\,^1\Delta)$ state, flow temperature, infrared spectra baseline and contribution of the atomic emission lines into the singlet delta emission intensity. From figure 11, it can be seen that the yield increases nearly proportionally to the discharge power, up to approximately 5.7% at $P_0 = 60$ Torr, 1.4 kW, and up to 5.0% at $P_0 = 120$ Torr, 2.1 kW. Note that at the same discharge power, SDO yield at $P_0 = 60$ Torr is approximately twice as high as at $P_0 = 120$ Torr (see figure 11). This shows that when the O_2 fraction in the flow is kept the same, the yield scales nearly proportionally to the specific power, i.e. the ratio of the discharge power to the flow rate through the discharge. SDO yield measurements in three different oxygen–helium mixtures at $P_0 = 120$ Torr, with 10%, 15% and 20% oxygen fraction, at the same dc voltage of $U_{PS} = 2.5$ kV (discharge power 1.2–1.4 kW) showed that increasing the oxygen mole fraction in the mixture weakly affects the yield, which remained about the same, in the range 2.1–2.8%. This suggests that the present approach can be used to obtain SDO yields up to 5–6% in O_2–He mixtures with up to 20% oxygen fraction, which may significantly increase the power stored in SDO.

The highest SDO yield measurements at two different stagnation pressures are summarized in table 1. The power stored in SDO, $\dot{Q}_{SDO}$, was calculated from the SDO flow rate, $\dot{n}_{SDO}$, as follows, $\dot{Q}_{SDO} = \dot{n}_{SDO} \cdot N_A \cdot \varepsilon_{SDO}$, where N_A is the Avogadro number and $\varepsilon_{SDO} = 0.96$ eV is the SDO energy. The results of table 1 show that at the flow temperatures achieved at the end of the $M = 3$ cavity, $T = 120$ K, the measured

Table 1. Summary of SDO measurements in a 10% O_2–He $M = 3$ flow.

P_0 (Torr)	T_0 (K)	Discharge power (kW)	P_{cavity}, (Torr)	M_{cavity}	T_{cavity} (K)	SDO yield (%)	Threshold yield (%)	Power stored in SDO (W)
60	400 ± 25	1.6	1.9	3.0	120 ± 15	5.7 ± 0.85	2.3	110
120	400 ± 25	2.1	3.8	3.0	120 ± 15	5.0 ± 0.75	2.3	200

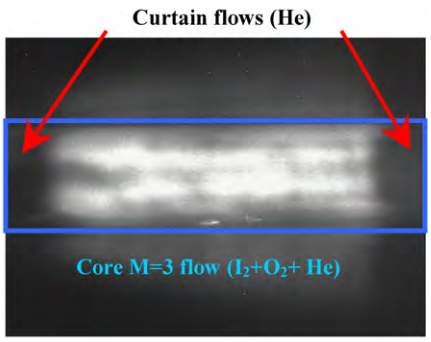

Figure 12. I_2 vapour PLIF flow image in the $M = 3$ cavity, averaged over 100 laser pulses. The flow is out of the page. An approximate outline of the rectangular test section is also shown.

SDO yields exceed gain threshold yields for these temperatures by up to a factor of 2.5. Therefore, the results suggest that yields measured at the present conditions, although relatively low (5.0–5.7%), may be sufficient for achieving positive gain in the low-temperature supersonic cavity. This implies that more than half of the power stored in the SDO flow at these conditions, 110 W (SDO flow rate at $P_0 = 60$ Torr of 1.25 mmol s^{-1}) and 200 W (SDO flow rate at $P_0 = 120$ Torr of 2.2 mmol s^{-1}), may be available for coupling out as laser power.

From table 1, it can be seen that the SDO generation efficiency by the discharge, i.e. the ratio of the power stored in SDO to the sustainer discharge power, increases with pressure. At $P_0 = 60$ Torr, $\approx$ 7% of the discharge power is stored in SDO, compared with $\approx$ 9.5% at $P_0 = 120$ Torr (see table 1). This behaviour is consistent with lower E/N values measured at $P_0 = 120$ Torr (see figure 8), at which the predicted fraction of the discharge power spent on SDO excitation increases [1, 3, 4, 12]. This result demonstrates key advantage of operating the pulser-sustainer discharge at high pressure, on condition that the discharge stability can be maintained.

Figure 12 shows a typical average I_2 PLIF image, which is a summation of 100 instantaneous (single laser pulse) images. The vertical field-of-view spans approximately three times the cavity height and the horizontal field-of-view spans the entire width of the cavity. A helium flow seeded with iodine vapour heated approximately to 40 °C is injected transversely, at an upstream location corresponding to $M \sim 0.5$ (see figure 1). Two 1 cm wide helium curtain flows are added to the 5 cm wide core flow on both sides, such as shown in figure 3, which are intended to protect the resonator arms and the laser mirrors (see section 2). Note that the iodine vapour/helium flow is delivered to the injector blocks from the right, and the flow through the injector blocks is right to left. From figure 12, it can be seen that the curtain flow regions 5 cm downstream of the nozzle exit plane remain essentially iodine-free. However, the core flow exhibits large-scale structures, detectable even in the time-average image, and a region adjacent to the left curtain flow lacks iodine. Clearly, iodine vapour mixing with the core oxygen–iodine flow needs improvement. The design of new iodine injector blocks with two rows of staggered injector holes of different diameters is currently underway.

4. Summary

The paper presents results of a high-pressure, non-self-sustained crossed discharge/$M = 3$ supersonic laser cavity operation. A stable and diffuse pulser-sustainer discharge in O_2–He flows is generated at pressures of up to $P_0 = 120$ Torr and discharge powers of up to 2.1 kW. The reduced electric field in the dc sustainer discharge ranges from 0.6×10^{-16} to 1.2×10^{-16} V cm^2. SDO yield in the discharge, up to 5.0–5.7% at the flow temperatures of 400–420 K, was inferred from the integrated intensity of the (0,0) band of the $O_2(a\,^1\Delta \rightarrow X\,^3\Sigma)$ infrared emission spectra calibrated using a blackbody source. The yield increases with the discharge power and remains nearly independent of the O_2 fraction in the mixture (in the 10–20% range). As was shown in our previous work [12], higher SDO yields can be obtained by increasing the flow residence time in the discharge (currently about 1 ms), e.g. by increasing the length of the discharge electrodes in the streamwise direction. Static pressure and temperature measurements in a supersonic cavity show that a steady-state $M = 3$ flow in the cavity can be sustained for up to 20 s, at the flow temperature of $T = 120 \pm 15$ K. The results suggest that the measured SDO yield exceeds the threshold yield at the cavity temperature by up to a factor of 2.5. This implies that more than half of the power stored in the SDO flow at these conditions, 110 W at $P_0 = 60$ Torr and 200 W at $P_0 = 120$ Torr, may be available for coupling out as laser power. PLIF iodine vapour visualization in the supersonic cavity, which showed the presence of large-scale structures, suggests the need to improve iodine mixing with the main oxygen–helium flow. Small signal gain measurements in the laser cavity and laser output power are currently underway. Recently, both positive gain and cw laser power output have been demonstrated using the present experimental facility [24]. These recent results will be presented in a separate paper.

Acknowledgments

This work was supported by a Phase II STTR sponsored by the Missile Defense Agency and the Directed Energy Directorate, Air Force Research Laboratory, Kirtland AFB, NM, under a subcontract from Physical Sciences, Inc., and by the Joint Technology Office. We would like to express our sincere gratitude to Drs Tim Madden, Gordon Hager and Tony Hostutler of AFRL, Drs Wayne Solomon and Dave Carroll of CU Aerospace, Drs Steve Davis, Bill Kessler and Kristine Galbally-Kinney from PSI and Sergey Gorbatov of Chemical Physics Technologies for helpful discussions during this work.

References

[1] Napartovich A P, Deryugin A and Kochetov I 2001 Discharge production of the singlet delta oxygen for an iodine laser *J. Phys. D: Appl. Phys.* **34** 1827–33

[2] Schmiedberger J and Fujii H 2001 Radio-frequency plasma jet generator of singlet delta oxygen with high yield *Appl. Phys. Lett.* **78** 2649–51

[3] Ionin A A, Klimachev Y M, Kotkov A A, Kochetov I V, Napartovich A P, Seleznev L V, Sinitsyn D V and Hager G D 2003 Non-self-sustained electric discharge in oxygen gas mixtures: singlet delta oxygen production *J. Phys. D: Appl. Phys.* **36** 982–9

[4] Vagin N P, Ionin A A, Klimachev Yu M, Kochetov I V, Napartovich A P, Sinitsyn D V and Yuryshev N N 2003 Glow discharge in singlet oxygen *Plasma Phys. Rep.* **29** 211–9

[5] Vasiljeva A N, Klopovskiy K S, Kovalev A S, Lopaev D V, Mankelevich Y A, Popov N A, Rakhimov A T and Rakhimova T V 2004 On the possibility of $O_2(a\,^1\Delta)$ production by a non-self-sustained discharge for oxygen–iodine laser pumping *J. Phys. D: Appl. Phys.* **37** 2455–68

[6] Carroll D L, Verdeyen J T, King D M, Zimmerman J W, Laystrom J K, Woodard B S, Richardson N, Kittell K, Kushner M J and Solomon W C 2004 Measurement of positive gain on the 1315 nm transition of atomic iodine pumped by $O_2(a\,^1\Delta)$ produced in an electric discharge *Appl. Phys. Lett.* **85** 1320–2

[7] Carroll D L, Verdeyen J T, King D M, Zimmerman J W, Laystrom J K, Woodard B S, Benavides G F, Kittell K W and Solomon W C 2005 Path to the measurement of positive gain on the 1315 nm transition of atomic iodine pumped by $O_2(a\,^1\Delta)$ produced in an electric discharge *IEEE J. Quantum Electron.* **41** 213–23

[8] Braginskiy O V, Vasilieva A N, Klopovskiy K S, Kovalev A S, Lopaev D V, Proshina O V, Rakhimova T V and Rakhimov A T 2005 Singlet oxygen generation in O_2 flow excited by RF discharge: I. Homogeneous discharge mode: α-mode *J. Phys. D: Appl. Phys.* **38** 3609–25

[9] Braginskiy O V, Vasilieva A N, Kovalev A S, Lopaev D V, Mankelevich A Yu, Rakhimova T V and Rakhimov A T 2005 Singlet oxygen generation in O_2 flow excited by RF discharge: II. Inhomogeneous discharge mode: plasma jet *J. Phys. D: Appl. Phys.* **38** 3626–34

[10] Carroll D L *et al* 2005 Continuous-wave laser oscillation on the 1315 nm transition of atomic iodine pumped by $O_2(a\,^1\Delta_g)$ produced in an electric discharge *Appl. Phys. Lett.* **86** 111104–3

[11] Rawlins W T, Lee S, Kessler W J and Davis S J 2005 Observations of gain on the transition $I(^2P_{1/2} \rightarrow {}^2P_{3/2})$ by energy transfer from $O_2(a^1\Delta_g)$ generated by a microwave discharge in a subsonic-flow reactor *Appl. Phys. Lett.* **86** 051105–3

[12] Hicks A, Norberg S, Shawcross P, Lempert W R, Rich J W and Adamovich I V 2005 Singlet oxygen generation in a high pressure non-self-sustained electric discharge *J. Phys. D: Appl. Phys.* **38** 3812–24

[13] King D M, Carroll D L, Verdeyen J T, Laystrom J K, Benavides G F, Palla A D, Zimmerman J W, Woodard B S and Solomon W C 2006 Power enhancement of the hybrid electricOIL laser *37th AIAA Plasmadynamics and Lasers Conf. (San Francisco, CA June 2006) AIAA Paper* 2006–3756

[14] Hon J, Plummer D N, Crowell P G, Erkkila J, Hager G D, Helms C and Truesdell K 1996 Heuristic method for evaluating coil performance *AIAA J.* **34** 1595

[15] Raizer Y P 1991 *Gas Discharge Physics* (Berlin: Springer)

[16] Hill A E 1973 Continuous uniform excitation of medium-pressure CO_2 laser plasmas by means of controlled avalanche ionization *Appl. Phys. Lett.* **22** p 670

[17] Generalov N A, Zimakov V P, Kosynkin V D, Raizer Yu P and Roitenburg D I 1975 Method for significantly increasing the stability limit of the discharge in fast-flow large-volume lasers *Tech. Phys. Lett.* **1** 201

[18] Nishihara M, Jiang N, Rich J W, Lempert W R, Adamovich I V and Gogineni S 2005 Low-temperature supersonic boundary layer control using repetitively pulsed MHD forcing *Phys. Fluids* **17** 106102

[19] Nishihara M, Rich J W, Lempert W R, Adamovich I V and Gogineni S 2006 Low-temperature $M = 3$ flow deceleration by Lorentz force *Phys. Fluids* **18** 086101

[20] Lou G, Bao A, Nishihara M, Keshav S, Utkin Y G, Rich J W, Lempert W R and Adamovich I V 2007 Ignition of premixed hydrocarbon-air flows by repetitively pulsed, nanosecond pulse duration plasma *Proc. Combustion Institute* vol 31 (January 2007) pp 3327–34

[21] Davis S J and Hanko L 1979 An I_2 flow rate diagnostic for the oxygen iodine laser *Laser Digest* AFWL-TR-79-104 (Air Force Weapons Laboratory, Kirtland AFB, New Mexico)

[22] Newman S M, Lane I C, Orr-Ewing A J, Newnham D A and Ballard J 1999 Integrated absorption intensity and Einstein coefficients for the $O_2(a\,^1\Delta_g \rightarrow X^3\Sigma_g^-)$ (0,0) transition: a comparison of cavity ringdown and high resolution Fourier transform spectroscopy with a long-path absorption cell *J. Chem. Phys.* **110** 10749–57

[23] Lafferty J, Solodov A M, Lugez C L and Fraser G T 1998 Rotational line strength and self-pressure-broadening coefficients for the 1.27 μm $a^1\Delta_g \rightarrow X^3\Sigma_g^- v = 0 \rightarrow 0$ band of O_2 *Appl. Opt.* **37** 2264

[24] Hicks A, Tirupathi S, Utkin Y, Lempert W R, Rich J W, Adamovich I V, Kessler W J, Galbally-Kinney K, Rawlins W T and Davis S J 2006 Development of a pulser-sustainer electric discharge pumped oxygen-iodine laser *16th Int. Symp. on Gas Flow and Chemical Lasers & High Power Laser Conf. (GCL/HPL 2006) (Gmunden, Austria, 4–8 September 2006)*